Polymer Journal (2019) 51:501–509
https://doi.org/10.1038/s41428-018-0161-4

ORIGINAL ARTICLE

A porous chitosan nanofiber-poly(ethylene glycol) diacrylate hydrogel for metal adsorption from aqueous solutions

Sachiko Nitta[1] · Miki Akagi[2] · Hiroyuki Iwamoto[1,2]

Received: 12 September 2018 / Revised: 28 November 2018 / Accepted: 30 November 2018 / Published online: 8 January 2019

Abstract

Porous hydrogels for the adsorption of metals from aqueous solutions were prepared from chitosan nanofibers (CNFs) and poly(ethylene glycol) diacrylate (PEGDA). These hydrogels exhibited high swelling rates and porosities, which were evaluated by a gravimetric method and scanning electron microscopy, respectively. Both factors were influenced by the CNF/PEGDA ratio. The prepared hydrogels adsorbed both transition metals (e.g., copper) and post-transition metals (e.g., tin). The adsorption capacity increased with increasing CNF/PEGDA ratio, indicating synergism between chelation and the enlarged surface area of the porous structure during adsorption. The kinetic data indicated that metal adsorption could be fit to a pseudo-second-order kinetic model, whereas the equilibrium data were fit to the Langmuir isotherm model. Overall, the results revealed that CNF-PEG hydrogels are promising adsorbent materials for metal recovery in environmental applications.

Introduction

Water pollution caused by the release of metals from industrial activities is a serious threat to both human health and the environment; consequently, suitable metal-recovery techniques are required for environmental applications. Several adsorbents have been developed for the removal of metals, such as sludge, plant waste, resins, and zeolites. As a biomass-based adsorbent, chitosan has also attracted significant attention for the removal of heavy metals [1–6]. Chitosan is a non-toxic, biodegradable polysaccharide found in the biomass and is obtained from the partial deacetylation of chitin derived as a natural resource. The positive charge of the chitosan backbone is determined by the degree of chitin deacetylation and influences the adsorption ability of this material. Indeed, chitosan has been identified as an excellent natural adsorbent for metal ions owing to the amino ($–NH_2$) and hydroxyl (–OH) groups present on its backbone, and its metal-binding capacity is dependent on the chelation of these functional groups to metal ions [7, 8]. However, as a result of the solubility of chitosan in dilute mineral and organic acids [9], chemical or physical modification of chitosan is required to improve its stability. For example, semi-interpenetrating networks [10], molecular-imprinting polymers [11], magnetic nanoparticles [7], and polymer-grafted chitosan [12] have been used to modify chitosan. As a result, metal adsorption using chitosan-based materials has been reported for the removal of Cu, Cd, Hg, Zn, Pb, and Ni [2–5, 13–15].

Porous hydrogels are particularly effective at enhancing the metal-adsorption efficiency of chitosan in aqueous solutions owing to their high swelling properties and large specific surface areas [15–20]. However, the formation of hydrogels from chitosan requires the reaction of the backbone amino groups with crosslinkers such as aldehydes and maleic anhydrides, which, unfortunately, reduces the chelating capacity of chitosan. The development of a novel method for the formation of chitosan-based hydrogels that does not affect the chelating capacity of the adsorbent is therefore required. In this context, we previously reported the formation of a microporous hydrogel, namely a chitosan nanofiber-polyethylene-glycol hydrogel (CNF-PEG hydrogel), through a one-step chemical crosslinking reaction of poly(ethylene glycol) diacrylate (PEGDA) with CNFs (30–50 nm diameter, 2 μm length), without reacting the

✉ Sachiko Nitta
nitta@fubac.fukuyama-u.ac.jp

[1] Research Center for Green Science, Fukuyama University, Hiroshima 279-0292, Japan

[2] Department of Biotechnology, Faculty of Life Science and Biotechnology, Fukuyama University, Hiroshima 729-0292, Japan

amino groups of chitosan and without the use of a porogen [21].

Here, we report a study of the metal-adsorbing abilities of CNF-PEG hydrogels. As CNF-PEG hydrogels have microporous structures and, consequently, high surface areas and high responsiveness to water swelling, they are expected to possess high metal-adsorbing capacities. The effect of the CNF/PEGDA ratio on the swelling properties and porosities of such hydrogels has yet to be examined in detail, despite knowing that physical and chemical properties significantly influence the adsorption capacity [8]. We therefore aimed to explore the effect of the chemical compositions of CNF-PEG hydrogels on their physical properties, such as porosity, swelling rate, and adsorption capacity. To the best of our knowledge, this is the first comprehensive study of the applicability of CNF-based hydrogels as metal-adsorption agents.

Materials and methods

Materials

A 10-wt% suspension of CNF (polymerization degree = 480, degree of deacylation ≥80%) in water and chitosan powder (polymerization degree = 480, degree of deacylation ≥80%) were purchased from Sugino Machine, Ltd. (Toyama, Japan) and used as received. Ammonium persulfate (APS), *N,N,N′,N′*-tetramethylethylenediamine (TEMED), and a copper standard solution (1000 g/L, in 5% HNO_3) were purchased from Wako Pure Chemical Industries, Ltd. (Tokyo, Japan). PEGDA (molecular weight = 800 Da) was purchased from Sigma-Aldrich (St. Louis, MO, USA). A metal standard solution (10ppm) containing a selection of 32 metals and metalloids (XSTC-622) was purchased from SPEX CertiPrep (NJ, USA). All chemicals were of analytical grade and used as received.

Preparation of CNF-PEG hydrogels

A series of CNF-PEG hydrogels were prepared as described previously [21]. More specifically, PEGDA (300 mg) was first weighed in a 6.5-mm-diameter cylindrical container. A suspension of CNF (10 wt% in water, 3.0 g) and deionized water (2.0 g) was then added to the container and mixed vigorously. After an aqueous solution of APS (200 mg, 40 mg/mL) was added to the mixture, TEMED (20 mg) was added and mixed thoroughly. The mixture was immediately incubated at 25 °C for 1 h to obtain the bulk hydrogel. The obtained hydrogel was sliced into 6.0-mm-thick portions, washed twice with deionized water, and lyophilized. The CNF/PEGDA ratio was calculated using the following equation:

CNF/PEGDA ratio = (weight of CNF suspension) × 0.1/(weight of PEGDA).

Chitosan powder gels were prepared as follows: PEGDA (300 mg), chitosan powder (300 mg), and APS (200 mg, 40 mg/mL) were mixed in deionized water (4.7 g). Then, TEMED (20 mg) was added and mixed thoroughly. The mixture was immediately incubated at 25 °C for 1 h to obtain the bulk hydrogel. The obtained hydrogel was sliced into 6.0-mm-thick portions, washed twice with deionized water, and lyophilized.

Characterization of the CNF-PEG hydrogels

The chemical structures of the CNF-PEG hydrogels were analyzed by attenuated total reflection/Fourier transform infrared spectroscopy (FT-IR, FT-720, HORIBA, Japan). The spectra were obtained with 64 scans per sample, with a range of 2000 to 500 cm^{-1}.

The morphologies of the CNF-PEG hydrogels were examined by scanning electron microscopy (SEM) on a scanning electron microscope equipped with a cooling stage (S-3400N, Hitachi, Japan). More specifically, the cylindrical CNF-PEG hydrogels were cross-sectioned into 5 mm × 5 mm squares with a thickness of 2 mm. SEM was conducted on the uncoated samples at an accelerating voltage of 8.00 kV under a vacuum of 70 Pa at −25 °C. The obtained images (×250magnification) were processed using Adobe Photoshop CS (Adobe, San Jose, CA, USA) to calculate the porosities of the CNF-PEG hydrogels prepared using a range of CNF/PEGDA ratios. In these images, the dark areas corresponded to pores formed by PEGDA crosslinking in the presence of CNF, whereas the white areas corresponded to the skeletal structure of the CNF-PEG hydrogel. The total number of pixels in the black and white areas was determined using the "magic wand" function of Photoshop (i.e., by selecting similar colors and counting the pixels within the selected area) in the histogram display [22, 23]. Porosity was calculated using the following equation:

Porosity (%) = (number of pixels in black area/total number of pixels in the image) × 100.

Swelling kinetics

The classical gravimetric method was used to study the swelling kinetics of the CNF-PEG hydrogels. The lyophilized hydrogels were immersed in acetic acid buffer (pH 4.0, 0.2 M), and samples were removed for analysis at set times over a period of 1 h. After weighing each CNF-PEG sample, the swelling degree was calculated using the following equation:

$$\text{Swelling degree}(\text{g}/\text{g}) = W_{t=t'}/W_{\text{dry}},$$

where $W_{t=t'}$ and W_{dry} indicate the weights of the gels at $t = t'$ (min) and the dried gel, respectively. The data were then fit to the following first-order kinetics equation:

$$\ln(1 - q_t/q_{ms}) = -k_s t,$$

where q_t and q_{ms} are the quantities of buffer taken up by the CNF hydrogel at time t and at equilibrium, respectively, and k_s is the pseudo-first-order swelling rate constant. The relationship between $-\ln(1-q_t/q_{ms})$ and t provides the value of k_s at each CNF/PEGDA ratio. All experiments were repeated in triplicate ($n = 3$).

Performance of the CNF-PEG hydrogels in adsorption experiments

Adsorption of metals in a standard solution

The adsorption of a variety of metals by the CNF-PEG hydrogel was initially examined using a mixed standard solution containing 32 different metals. Mixed metal standard solutions containing initial concentrations of each metal ion of 1 mg/L were prepared by diluting the 10 mg/L standard metal solution (in 5% HNO_3) with deionized water and adjusting the pH of these solutions to 4.0 using a 0.1 mol/L NaOH solution. Unless otherwise stated, CNF-PEG hydrogels with a CNF/PEGDA ratio of 1.0 were used in all adsorption experiments. Uptake experiments were performed by placing the lyophilized CNF-PEG hydrogels in Falcon tubes containing the metal standard solutions (50 mL, 1.0 mg/L) at pH 4.0. The sample tubes were agitated at 100 rpm using a shaker for ≤48 h at 25 °C. Aliquots were removed from the solutions at the desired intervals, and the metal concentrations in each solution were determined by inductively coupled plasma (ICP) optical emission spectrometry (ICP-OES, SPS5100, Hitachi, Japan).

Adsorption experiments

To determine the copper-adsorption abilities of the CNF-PEG hydrogels, a solution of Cu with an initial concentration of 10 mg/L was prepared by diluting the 1000 mg/L standard Cu solution (in 5% HNO_3) with deionized water and adjusting the pH to 4.0 using a 0.1 mol/L solution of NaOH. Uptake experiments were performed by placing the lyophilized CNF-PEG hydrogels in Falcon tubes containing the Cu-ion solution (50 mL, 10 mg/L) at pH 4.0. The sample tubes were agitated at 100 rpm using a shaker for ≤48 h at 25 °C. Aliquots were removed from the solutions at the desired intervals, and the Cu concentration of each solution was determined by ICP.

The quantity of metal ions adsorbed per unit mass of CNF-PEG hydrogel (mg/g) was calculated based on the following mass-balance equation:

$$q = \left(C_0 - C_{eq}\right) \times V/m,$$

where q is the adsorption capacity (mg/g), C_0 is the initial concentration of Cu in the solution at $t = 0$ (min) (mg/L), C_{eq} is the equilibrium concentration of Cu in the solution (mg/L), V is the volume of the solution (L), and m is the weight of the dried CNF-PEG hydrogel (g).

For the adsorption kinetics studies, the lyophilized CNF-PEG hydrogels were placed in sample tubes containing the Cu-ion solution (50 mL, 10 mg/L) at pH 4.0. The sample tubes were agitated at 100 rpm using a shaker for ≤48 h at 15, 25, 35, or 45 °C. During the kinetics experiments, aliquots were removed from the samples at fixed intervals, and the concentration of Cu ions in each sample was determined. The adsorption isotherms of the CNF-PEG hydrogels were subsequently determined at various initial Cu-ion concentrations (10–1000 mg/L) and pH 4.0.

The effect of the CNF/PEGDA ratio on hydrogel adsorption

Uptake experiments were carried out using dry CNF-PEG hydrogels with CNF/PEGDA ratios of 0.6–1.5 (g/g). Briefly, PEGDA (200–500 mg), a suspension of CNF (10 wt% in water, 3.0 g) and deionized water (2.0 g) were weighed in a 6.5-mm-diameter cylindrical container and mixed vigorously. After an aqueous solution of APS (200 mg, 40 mg/mL) was added to the mixture, TEMED (20 mg) was added and mixed thoroughly. The mixture was immediately incubated at 25 °C for 1 h to give the bulk hydrogel. The obtained hydrogel was sliced into 6.0-mm-thick portions, washed twice with deionized water, and lyophilized. Each CNF-PEG hydrogel was placed in Falcon tubes containing the Cu-ion solution (50 mL, 10 mg/L) at pH 4.0. The sample tubes were agitated at 100 rpm using a shaker for ≤48 h at 25 °C. Aliquots were removed from the various solutions at the desired time intervals, and the Cu concentrations were determined by ICP.

The effect of adsorption conditions

The effect of pH on the adsorption of Cu ions by the CNF-PEG hydrogels was examined in a pH range of 3.0–6.0 at 25 °C. The solution pH was adjusted to the desired value using 1.0 M solutions of NaOH and HCl. Uptake experiments were performed by placing the lyophilized CNF-PEG hydrogels in Falcon tubes containing the Cu-ion solution (50 mL, 10 mg/L) at the pH values of interest. The sample tubes were agitated at 100 rpm using a shaker for ≤48 h at 25 °C. Aliquots were removed from each solution at the desired intervals, and the Cu concentrations were determined by ICP.

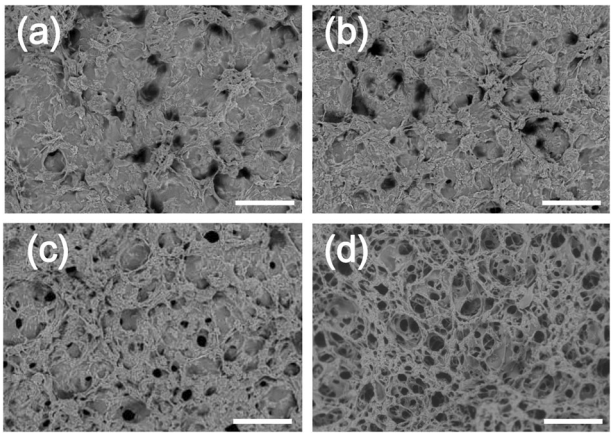

Fig. 1 SEM images of CNF-PEG hydrogels with different CNF/PEGDA ratios: **a** 0.60, **b** 0.75, **c** 1.00, and **d** 1.50. All scale bars are 100 μm

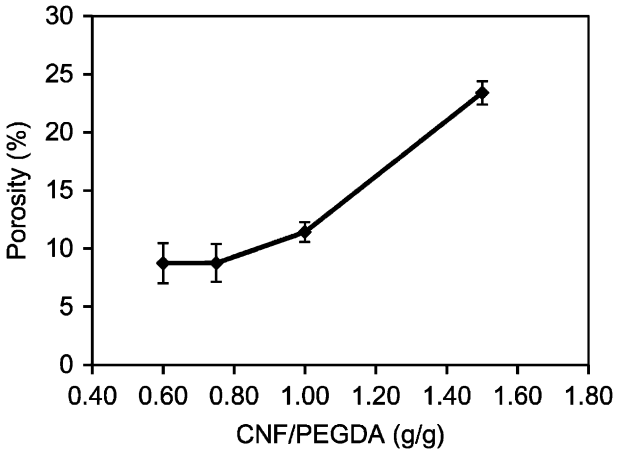

Fig. 2 Effect of CNF/PEGDA ratio on CNF-PEG-hydrogel porosity. CNF-PEG hydrogels were prepared with CNF/PEGDA ratios of 0.60, 0.75, 1.00, and 1.50. Porosity was calculated as the ratio of the pixels of the porous dark areas to the total numbers of pixels, as given in the SEM images (Fig. 1)

Results and discussion

Morphologies of the CNF-PEG hydrogels

Hydrogels are commonly employed as adsorbents for toxic metal ions due to their swelling properties. As high porosity, which ensures a sufficiently large specific surface area, is also important in this context, the factors that affect hydrogel porosity need to be clearly understood. Hence, we first examined the effect of the CNF/PEGDA ratio on the porosity of our CNF-PEG hydrogels. The CNF/PEGDA ratio was calculated from the amount of CNF in suspension and PEGDA measured before the crosslinking reaction, since the gel fractions of CNF-PEG hydrogels were as high as 90% regardless of the CNF/PEGDA ratio. In addition, we confirmed by FT-IR that the amino groups of chitosan (wavenumber of 1577 cm^{-1}) remained in the CNF-PEG hydrogels after the crosslinking reaction. Following their preparation, the morphology of each CNF-PEG hydrogel sample (i.e., with CNF/PEGDA ratios of 0.60, 0.75, 1.00, and 1.50) was examined by SEM, which confirmed the formation of microscale pores (Fig. 1). These results are in agreement with our previous report showing that PEGDA gelation aligned with the bundles of CNF, resulting in the formation of micropores [21]. To avoid water evaporation, the SEM observations were carried out with the specimens directly chilled on the cooling stage of the SEM at –25 °C under low vacuum. With this method, we were able to demonstrate the morphology of the CNF-PEG hydrogels during metal adsorption without micropore shrinking due to lyophilization. The uniform microporous structure was observed regardless of which sections of the gels were analyzed.

The porosity of each hydrogel sample was subsequently determined by calculating the ratios of the black and white pixels in the binary SEM images using Adobe Photoshop. The effect of the CNF/PEGDA ratio on the porosity of each hydrogel was calculated, the results of which are shown in Fig. 2. Since porosity was calculated from the SEM images, we surmised that the thickness of the gel slices could potentially affect the total numbers of pixels in the black and white areas due to the formation of multilayers in the CNF-PEG hydrogels. Thus, to avoid any effects due to thickness, the samples were sliced to the same thickness (2 mm) prior to SEM, irrespective of the type of sample.

Interestingly, porosity was observed to increase from 8.75 to 23.4% as the CNF/PEGDA ratio increased from 0.60 to 1.50 (Fig. 2). During the preparation of the hydrogel samples, a stable and highly viscous CNF suspension was blended with the PEGDA solution in deionized water, which trapped the CNFs within the PEGDA [21]. As a result, the CNFs were covered by PEGDA networks at low CNF/PEGDA ratios, whereas micropores formed easily at higher ratios by bridging CNF bundles through the intermolecular crosslinking of PEGDA. These results confirmed that the CNF-PEG hydrogels prepared using higher CNF/PEGDA ratios possessed greater numbers of pores with tighter network structures, thereby resulting in higher specific surface areas.

Swelling properties of the CNF-PEG hydrogels

We previously studied the swelling properties of CNF-PEG hydrogels in deionized water, in which the CNF was deprotonated. Here, we conducted swelling experiments involving the CNF-PEG hydrogels in an acetic acid buffer (pH 4.0) to determine the response kinetics of the porous hydrogels under conditions in which the CNF is positively charged. Hence, to examine the response behavior of the CNF-PEG hydrogels, the swelling rates of the hydrogels prepared using

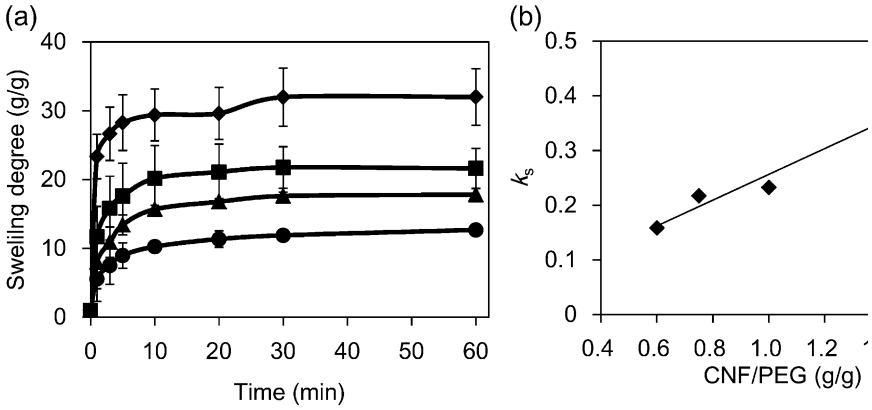

Fig. 3 **a** Swelling rates of CNF-PEG hydrogels prepared using different CNF/PEGDA ratios: solid circle 0.60, solid triangle 0.75, solid square 1.00, and solid rectange 1.50. **b** Pseudo-first-order swelling rate constant (k_s) as a function of the CNF/PEGDA ratio

various CNF/PEGDA ratios were determined. As shown in Fig. 3a, the CNF hydrogels exhibited rapid water-swelling responses and reached swelling equilibria within ~10 min. In this case, three main steps occurred during the swelling of the dried hydrogel in water: (1) water diffused into the stiffed polymer network; (2) the hydrated polymer chains then rapidly relaxed due to the hydrophilicity of PEGDA; and (3) the polymer network expanded into the surrounding water [17]. During such a swelling process, water must overcome the osmotic pressure inside the gel [24], and elastic forces then prevent deformation of the network against the osmotic force. Swelling is complete when the elastic and osmotic forces are in equilibrium. The highly connected and stable internal network of the CNF-PEG hydrogel in each sample examined here facilitated rapid convectional water transport both inwards and outwards, thereby resulting in rapid swelling [17].

As shown in Fig. 3a, the degree of swelling at equilibrium increased as the CNF/PEGDA ratio increased, likely due to decreasing PEGDA-crosslinking density [21]. Indeed, the loosely packed network structure of PEGDA at low crosslinking densities accommodates greater amounts of water in the hydrogel [17]. In addition, increases in the CNF/PEGDA ratio enhance the electrostatic interactions between the chitosan backbones, thereby increasing the overall swelling degree of the hydrogel [25].

We next examined the effect of the CNF/PEGDA ratio on the pseudo-first-order swelling rate constant (k_s), the results of which are shown Fig. 3b. In this case, the value of k_s increased with increasing CNF/PEGDA ratio. Indeed, it has been reported that hydrogels with higher specific surface areas and larger pore sizes have larger swelling rate constants and lower swelling activation energies due to their faster response behavior [24, 26]. In addition, the porosity increased with increasing CNF/PEGDA ratio (Fig. 2), which may explain the rapid response of the CNF-PEG hydrogels at higher CNF/PEGDA ratios. The diffusion coefficient (D_{eff}) can be expressed as follows [26, 27]:

$$D_{eff} = D_{iw} K_p \varepsilon / \tau,$$

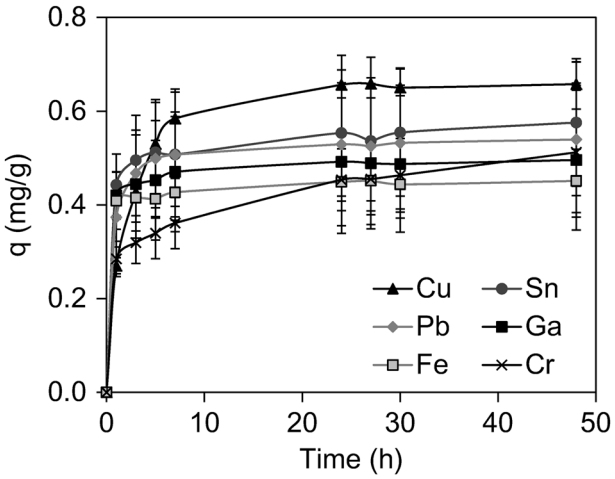

Fig. 4 Heavy metal adsorption on the CNF-PEG hydrogel as a function of time. The adsorption of metal ions on the CNF-PEG hydrogel with a CNF/PEGDA ratio of 1.0 was conducted using the metal standard solution (1.0 mg/L, pH 4.0) at 25 ℃

where D_{iw}, K_p, ε, and τ are the diffusion coefficient of the solute in the water-filled pores, the partition coefficient, the network porosity, and the network tortuosity, respectively. From this equation, we confirmed that increases in hydrogel porosity enhance the diffusion of water within the gel, resulting in an increase in the water-swelling rate.

Adsorption of metal ions from a standard metal solution

The adsorptions of various metal ions by the CNF-PEG hydrogel with a CNF/PEGDA ratio of 1.0 were next examined using a standard metal solution. As shown in Fig. 4, the CNF-PEG hydrogel not only adsorbed transition metals such as copper and iron but also post-transition metals such as tin, gallium, and lead. These results are consistent with literature data that confirm the adsorption of various heavy metals onto chitosan-based adsorbents [25, 28, 29]. By contrast, the CNF-PEG hydrogel exhibited low adsorbability toward molybdenum, zinc, manganese, alkali metals, and alkali-earth

metals. The adsorption capacities of metals on chitosan-based adsorbents have been reported to depend on adsorption conditions, such as buffer pH and HCl concentration, since the formation of a metal–chitosan complex is based on either electrostatic interactions or chelation [30]. Hence, the optimal adsorption capacities of each metal may be higher than the values obtained in this study. Nonetheless, it is worth noting that the CNF-PEG hydrogels exhibited adsorbability towards several types of metals even though chitosan in suspended rather than solution form during the adsorption process, which may hinder the formation of metal–chitosan complexes through electrostatic interactions or chelation. The adsorbabilities of metals on PEGDA hydrogels with no CNF and chitosan powder-PEG hydrogels were determined in the same manner used for the CNF-PEG hydrogels. These experiments confirmed that the PEGDA hydrogels had no adsorption ability, indicating that the presence of chitosan in the hydrogels is the critical factor for metal adsorption. Moreover, the CNF-PEG hydrogels had higher adsorption capacities than the chitosan powder-PEG hydrogels, indicating that the enhanced metal adsorbabilities were due to the larger specific surface areas of the CNF-PEG hydrogels compared with those of the chitosan powder-PEG hydrogels. The porous structure of the CNF-PEG hydrogels remained intact after metal adsorption.

Adsorption kinetics

Copper was selected to evaluate hydrogel-adsorption performance because it is one of the most common heavy metals studied. The effect of temperature on the adsorption capacity of the CNF-PEG hydrogel with a CNF/PEGDA ratio of 1.0 was examined at 25, 35, and 45 °C in a 10 ppm Cu solution at pH 4. As shown in Fig. 5, adsorption equilibria were reached at ~5, 24, and >48 h at 25, 35, and 45 °C, respectively, indicating that this process is endothermic.

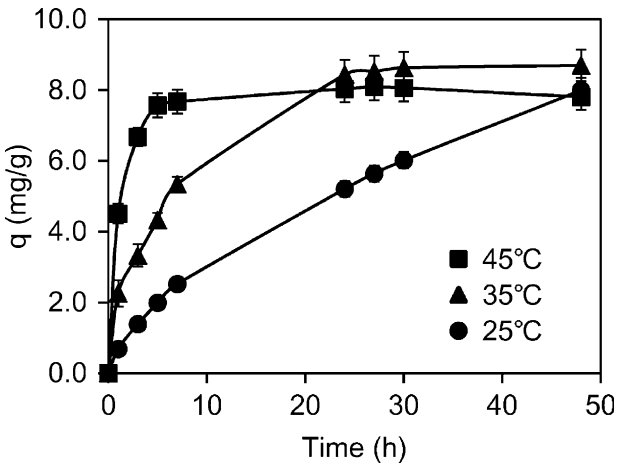

Fig. 5 Effect of temperature on the adsorption capacity of the CNF-PEG hydrogel with a CNF/PEGDA ratio of 1.0. Adsorption of Cu on the CNF-PEG hydrogel was conducted using a 10.0 mg/L copper solution (pH 4.0) at 25, 35, and 45 °C

Pseudo-first-order and pseudo-second-order kinetic models were then used to evaluate the mechanism controlling the adsorption of metal ions onto the CNF-PEG hydrogel; a good kinetic correlation can be used to determine the mechanism for metal ion adsorption onto the solid phase. The pseudo-first-order kinetic model is described by the following:

$$\ln(q_e - q_t) = \ln q_e - k_1 t,$$

where q_t and q_e (mg/g) are the adsorption capacities at time t and at equilibrium, respectively, and k_1 (min^{-1}) is the pseudo-first-order rate constant. Plots of $\ln(q_e - q_t)$ versus t at different temperatures provided values for the first-order rate constants (k_1) and the coefficient of determination (R^2) at 25, 35, and 45 °C, as shown in Table 1.

The pseudo-second-order kinetic model is described by the following:

$$t/q_t = t/q_e + 1/k_2 q_e^2,$$

where k_2 (g/mg·min) is the adsorption rate constant. Plots of t/q_t versus t at different temperatures gave values for the second-order rate constants (k_2) and the correlation coefficients (R^2) at 25, 35, and 45 °C. As shown in Table 1, the correlation coefficients for the pseudo-second-order model were higher than those for the pseudo-first-order model at 35 and 45 °C. The linear correlation method for determining the best-fit model suggests that the adsorption of Cu ions onto the CNF-PEG hydrogel follows a pseudo-second-order mechanism, which, in turn, suggests that the rate-controlling step involves chemisorption between the adsorbent surface and the metal ions rather than mass transfer in solution [19].

Adsorption isotherms

Adsorption isotherms provide a critical understanding of the interactions that take place between adsorbents and adsorbates. While many isotherms describe single-component adsorptions, metal adsorptions by hydrogels is commonly examined using the Langmuir and Freundlich isotherms. To

Table 1 Pseudo-first-order and pseudo-second-order rate data for Cu adsorption on the CNF-PEG hydrogels

Temperature (°C)	Q_{exp} (mg/g)	First-order model		Second-order model	
		k_1 (10^{-3} min^{-1})	R^2	k_2 (10^{-3}g/mg·min)	R^2
25	8.381	0.723	0.9967	0.134	0.9455
35	8.636	2.48	0.9954	0.508	0.9959
45	7.814	2.93	0.9067	7.75	0.9992

analyze the equilibrium data for Cu ions using these two adsorption isotherms, we adsorbed Cu onto our CNF-PEG hydrogels at initial ion concentrations of 10–150 mg/L.

Figure 6 shows the relationship between the adsorption capacity of the CNF-PEG hydrogel for Cu and the initial Cu concentration. More specifically, the adsorption capacity increased linearly with the initial Cu concentration at lower concentrations due to the presence of sufficient adsorption sites. In this case, the degree of adsorption depended on the number of Cu ions adsorbed from the solution onto the surface of the hydrogel. By contrast, the adsorption capacities did not increase linearly at higher initial Cu concentrations due to the presence of a limited number of adsorption sites on the hydrogel surface.

The general form of the Langmuir isotherm is expressed as follows:

$$C_e/q_e = 1/K_L q_m + C_e/q_m,$$

where q_e is the equilibrium quantity of metal ions adsorbed on the hydrogel, C_e is the equilibrium concentration (mg/L), and q_m (mg/g) and K_L (L/mg) are the Langmuir constants related to the saturation adsorption capacity and the binding energy, respectively. The Langmuir model indicates that the maximum adsorption capacity is achieved through monolayer adsorption, as no interactions between the adsorbed molecules and the adsorbent exist, and the adsorption energy is distributed homogenously over the surface. When a reaction site becomes occupied by a metal ion, no further adsorption occurs at that location; Fig. 7a displays the Langmuir plot, with the values of q_m, K_L, and R^2 obtained from the plot listed in Table 2.

By contrast, the Freundlich model is an empirical equation based on multilayer sorption on a heterogeneous surface and is commonly expressed as follows:

$$\ln q_e = \ln k_F + 1/n \ln C_e,$$

where k_F (mg/g) and n are the Freundlich constants related to the adsorption capacity and intensity of the sorbent, respectively; Fig. 7b displays the Freundlich plot, with the values of k_F and $1/n$ obtained from the equation listed in Table 2.

Comparison of the R^2 values obtained using the Freundlich ($R^2 = 0.976$) and Langmuir ($R^2 = 0.998$) models indicated that the adsorption of copper onto the CNF hydrogel follows the Langmuir isotherm model. In addition, we confirmed that the experimentally observed saturation capacities were close to the equilibrium adsorption capacities (q_m) obtained from the Langmuir model, which indicates that the monolayer Langmuir adsorption isotherm is a suitable model for the adsorption of Cu onto the hydrogel. Since chitosan-based adsorbents are often reported to conform to Langmuir adsorption isotherms, the adsorption capacities of the CNF hydrogels were considered to originate from the chitosan component.

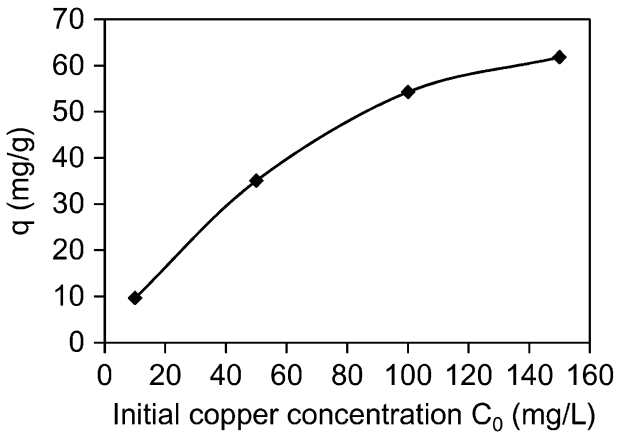

Fig. 6 Adsorption isotherm of Cu ions on the CNF-PEG hydrogel with a CNF/PEGFA ratio of 1.0. Adsorption of Cu on the CNF-PEG hydrogel was conducted using copper solutions with initial concentrations of 10, 50, 100, and 150 mg/L (pH 4.0) at 25 °C

Table 2 Langmuir and Freundlich isotherm data for adsorption of Cu ions on the CNF-PEG hydrogels

Langmuir			Freundlich		
Q_m (mg/g)	K_L (L/mg)	R^2	K_f (mg/g)	1/n	R^2
70.42	0.0833	0.998	0.0152	2.007	0.976

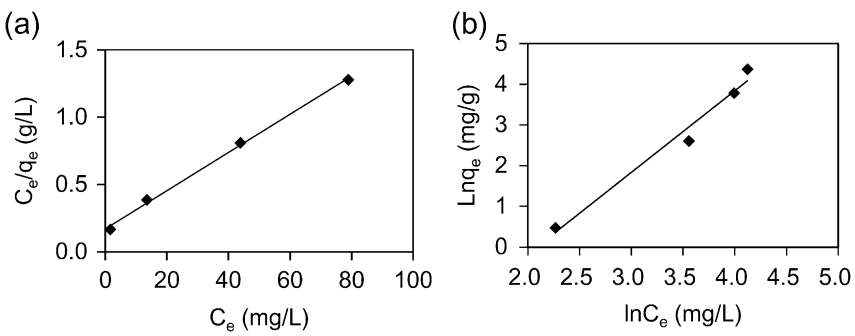

Fig. 7 **a** Langmuir and **b** Freundlich plots for Cu adsorption on the CNF-PEG hydrogel with a CNF/PEGDA ratio of 1.0

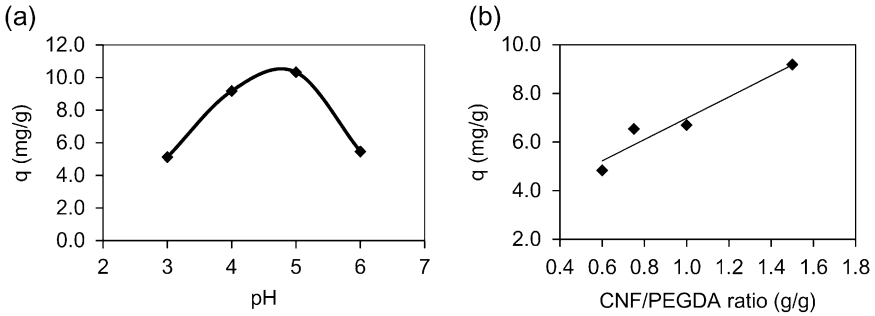

Fig. 8 **a** Effect of initial solution pH on the adsorption capacity of the CNF-PEG hydrogel with a CNF/PEGFA ratio of 1.0. Cu adsorption on CNF-PEG hydrogel was conducted in copper solutions (10.0 mg/L) at pH 3.0, 4.0, 5.0, and 6.0 at 25 °C. **b** Effect of the CNF/PEGDA ratio of the CNF-PEG hydrogel on the adsorption capacity of the CNF-PEG hydrogel. Cu adsorption on the CNF-PEG hydrogel was conducted in copper solution (10.0 mg/L) at pH 4.0 and 25 °C

The effects of pH and the CNF/PEGDA ratio

The effect of the initial pH on the adsorption capacity of the CNF-PEG hydrogel for Cu was studied over a pH range of 3–6 pH (Fig. 8a), which revealed that the adsorption of Cu ions (at an initial concentration of 10 mg/L) by the CNF-PEG hydrogel is indeed influenced by pH. At low pH values, the amino groups of the chitosan are in their protonated, positively charged forms; consequently, electrostatic repulsions between the metal cations and the protonated amino groups prevent metal ion adsorption onto the hydrogel surface [18, 28]. The adsorption capacity was observed to decrease due to Cu precipitation at pH values above 6.

Furthermore, the effect of the CNF/PEGDA ratio on the adsorption capacity of the CNF-PEG hydrogel was examined at CNF/PEGDA ratios of 0.60–1.50 (g/g). As shown in Fig. 8b, the adsorption capacity essentially doubled, from 4.84 to 9.18 (mg/g), as the CNF/PEGDA ratio increased from 0.60 to 1.50. This increase in adsorption capacity is ascribable to increases in not only the CNF ratio but also the porosity and, hence, the specific surface area (see Fig. 2) with increasing CNF/PEGDA ratio. It is therefore apparent that CNF exhibits synergism through the adsorption capacity of chitosan mediated by both chelation and the enlarged surface area of the porous structure. These results indicate that CNF is essential for the successful use of CNF-based hydrogels for metal-adsorption applications.

Conclusions

In this study, porous hydrogels based on CNFs and PEGDA were prepared for the adsorption of metal ions from aqueous solutions. We found that the porosities and swelling rates of these CNF hydrogels increased with increasing CNF/PEGDA ratio. In addition, the prepared hydrogels successfully adsorbed both heavy metals and metalloids from aqueous solutions, with optimal removal efficiency for Cu achieved at pH 4–5. Furthermore, the experimental data fit a pseudo-second-order kinetics model, indicating that chemical sorption is the rate-limiting step. Moreover, as the equilibrium data fit the Langmuir isotherm model, it is apparent that the presence of CNF enhances the adsorbability of chitosan due to chelation while also increasing the specific surface area of the porous structure, which synergistically increases the adsorption capacity of the gel. We also found that the adsorption capacity increases with increasing temperature, which suggests that the adsorption process is endothermic. Taken together, we expect that our results will facilitate the development of novel metal-recovery techniques for environmental applications such as those involving the removal of heavy metals from the mining and metal-plating industries.

Acknowledgements Dr Tatsuya Ikeda from the National Agriculture and Food Research Organization assisted with SEM. This work was supported by a Grant-in-Aid for JSPS Research Fellows under grant number 17J40043.

Compliance with ethical standards

Conflict of interest The authors declare no conflict of interest.

Publisher's note: Springer Nature remains neutral with regard to jurisdictional claims in published maps and institutional affiliations.

References

1. Guibal E. Interactions of metal ions with chitosan-based sorbents: a review. Sep Purif Technol. 2004;38:43–74.
2. Liu C, Bai R. Recent advances in chitosan and its derivatives as adsorbents for removal of pollutants from water and wastewater. Curr Opin Chem Eng. 2014;4:62–70.
3. Olivera S, Muralidhara HB, Venkatesh K, Guna VK, Gopalakrishna K, Kumar KY. Potential applications of cellulose and chitosan nanoparticles/composites in wastewater treatment: a review. Carbohydr Polym. 2016;153:600–18.

4. Zhang L, Zeng Y, Cheng Z. Removal of heavy metal ions using chitosan and modified chitosan: a review. J Mol Liq. 2016;214: 175–91.
5. Kandile NG, Nasr AS. Environment friendly modified chitosan hydrogels as a matrix for adsorption of metal ions, synthesis and characterization. Carbohydr Polym. 2009;78:753–9.
6. Xie M, Zeng L, Zhang Q, Kang Y, Xiao H, Peng Y, et al. Synthesis and adsorption behavior of magnetic microspheres based on chitosan/organic rectorite for low-concentration heavy metal removal. J Alloy Compd. 2015;647:892–905.
7. Gerente C, Lee VKC, Cloirec PL, McKay G. Application of chitosan for the removal of metals from wastewaters by adsorption —mechanisms and models review. Crit Rev Environ Sci Technol. 2007;37:41–127.
8. Jansson-Charrier M, Guibal E, Roussy J, Delanghe B, Le Cloirec P. Vanadium (IV) sorption by chitosan: kinetics and equilibrium. Water Res. 1996;30:465–75.
9. Wang W-B, Huang D-J, Kang Y-R, Wang A-Q. One-step in situ fabrication of a granular semi-IPN hydrogel based on chitosan and gelatin for fast and efficient adsorption of Cu^{2+} ion. Colloids Surf B. 2013;106:51–59.
10. Tianwei T, Xiaojing H, Weixia D. Adsorption behaviour of metal ions on imprinted chitosan resin. J Chem Technol Biotechnol. 2001;76:191–5.
11. Igberase E, Osifo P, Ofomaja A. The adsorption of copper (II) ions by polyaniline graft chitosan beads from aqueous solution: equilibrium, kinetic and desorption studies. J Environ Chem Eng. 2014;2:362–9.
12. Boamah PO, Huang Y, Hua M, Zhang Q, Wu J, Onumah J, et al. Sorption of heavy metal ions onto carboxylate chitosan derivatives—a mini-review. Ecotoxicol Environ Saf 116, 113-120. 2015;116:113–20.
13. Wang J, Chen C. Chitosan-based biosorbents: modification and application for biosorption of heavy metals and radionuclides. Bioresour Technol. 2014;160:129–41.
14. Desai K, Kit K, Li J, Davidson PM, Zivanovic S, Meyer H. Nanofibrous chitosan non-wovens for filtration applications. Polymer (Guildf). 2009;50:3661–9.
15. Wang X, Li Y, Li H, Yang C. Chitosan membrane adsorber for low concentration copper ion removal. Carbohydr Polym. 2016; 146:274–81.
16. Aliabadi M, Irani M, Ismaeili J, Piri H, Parnian MJ. Electrospun nanofiber membrane of PEO/chitosan for the adsorption of nickel, cadmium, lead and copper ions from aqueous solution. Chem Eng J. 2013;220:237–43.
17. Dang QF, Yan JQ, Li JJ, Cheng XJ, Liu CS, Chen XG. Controlled gelation temperature, pore diameter and degradation of a highly porous chitosan-based hydrogel. Carbohydr Polym. 2011;83:171–8.
18. Li N, Bai R. Copper adsorption on chitosan–cellulose hydrogel beads: behaviors and mechanisms. Sep Purif Technol. 2005;42: 237–47.
19. J-s Wang, R-t Peng, J-h Yang, Y-c Liu, Hu X-j. (2011). Preparation of ethylenediamine-modified magnetic chitosan complex for adsorption of uranyl ions. Carbohydr Polym. 2011;84:1169–75.
20. Peng X-W, Zhong L-X, Ren J-L, Sun R-C. Highly effective adsorption of heavy metal ions from aqueous solutions by macroporous xylan-rich hemicelluloses-based hydrogel. J Agric Food Chem. 2012;60:3909–16.
21. Nitta S, Kaketani S, Iwamoto H. Development of chitosan-nanofiber-based hydrogels exhibiting high mechanical strength and pH-responsive controlled release. Eur Polym J. 2015;67: 50–56.
22. Smith AL, Leung J, Kun S, Zhang R, Karagiannides I, Raz S, et al. The effects of acute and chronic psychological stress on bladder function in a rodent model. Urology. 2011;78:967. e961–967.e967.
23. Rimmelé G, Barlet-Gouédard V, Porcherie O, Goffé B, Brunet F. Heterogeneous porosity distribution in Portland cement exposed to CO_2-rich fluids. Cem Concr Res. 2008;38:1038–48.
24. Zhao ZX, Li Z, Xia QB, Bajalis E, Xi HX, Lin YS. (2008). Swelling/deswelling kinetics of PNIPAAm hydrogels synthesized by microwave irradiation. Chem Eng J. 2008;142:263–70.
25. Paulino AT, Belfiore LA, Kubota LT, Muniz EC, Almeida VC, Tambourgi EB. Effect of magnetite on the adsorption behavior of Pb(II), Cd(II), and Cu(II) in chitosan-based hydrogels. Desalination. 2011;275:187–96.
26. Ganji F, Vasheghani-Farahani S, Vasheghani-Farahani E. Theoretical description of hydrogel swelling: a review. Iran Polym J. 2010;19:375–298.
27. Wallmersperger T, Wittel FK, D'Ottavio M, Kröplin B. Multiscale modeling of polymer gels—chemo-electric model versus discrete element model. Mech Adv Mater Struct. 2008; 15:228–34.
28. Monier M. Adsorption of Hg^{2+}, Cu^{2+} and Zn^{2+} ions from aqueous solution using formaldehyde cross-linked modified chitosan–thioglyceraldehyde Schiff's base. Int J Biol Macromol. 2012;50: 773–81.
29. Copello GJ, Varela F, Vivot RM, Díaz LE. Immobilized chitosan as biosorbent for the removal of Cd(II), Cr(III) and Cr(VI) from aqueous solutions. Bioresour Technol. 2008;99:6538–44.
30. Inoue K, Baba Y, Yoshizuka K. Adsorption of metal ions on chitosan and crosslinked copper(II)-complexed chitosan. Bull Chem Soc Jpn. 1993;66:2915–21.